*fluids*

MDPI

*Article*

# Magneto-eklinostrophic Flow, Electromagnetic Columns, and von Kármán Vortices in Magneto-Fluid Dynamics

**Peter Vadasz**

Department of Mechanical Engineering, Northern Arizona University, Flagstaff, AZ 86011, USA; peter.vadasz@nau.edu

**Abstract:** An analogy between magneto-fluid dynamics (MFD/MHD) and geostrophic flow in a rotating frame of reference, including the existence of electromagnetic columns identical to Taylor–Proudman columns, is identified and demonstrated theoretically here. The latter occurs within the limit of large values of a dimensionless group representing the magnetic field number. Such conditions are shown to be easily satisfied in reality. Consequently, the electromagnetic fluid flow subject to these conditions is two dimensional and the streamlines are shown to be identical to the pressure lines, in complete analogy to rotating geostrophic flows. These results suggest that von Kármán vortices are anticipated in the wake of virtual electromagnetic columns. An experimental setup is suggested to confirm the theoretical results experimentally.

**Keywords:** magneto-eklinostrophic flow; electromagnetic columns; Taylor–Proudman columns; geostrophic flow

check for updates

**Citation:** Vadasz, P. Magneto-eklinostrophic Flow, Electromagnetic Columns, and von Kármán Vortices in Magneto-Fluid Dynamics. *Fluids* **2024**, *9*, 242. https://doi.org/10.3390/fluids9100242

Academic Editors: Sergey Smolentsev and D. Andrew S. Rees

Received: 20 August 2024
Revised: 5 October 2024
Accepted: 16 October 2024
Published: 18 October 2024

**Copyright:** © 2024 by the author. Licensee MDPI, Basel, Switzerland. This article is an open access article distributed under the terms and conditions of the Creative Commons Attribution (CC BY) license (https://creativecommons.org/licenses/by/4.0/).

## 1. Introduction

The flow of electric charges within or with a fluid, or alternatively freely moving in free space, is currently being analyzed as a part of magneto-fluid dynamics (MFD). The latter appears also under the acronym MHD (magneto-hydrodynamics), although this is inaccurately linked to water (hydro) flow due to historical reasons. It applies to plasmas and liquid metals, as well as beams of charges moving in free space. The present paper deals with the theoretical demonstration of two linked MFD effects that have been shown to be analogous to fluid flow in a rotating frame of reference. The flow of fluids in a rotating frame of reference has been studied extensively and has applications in geophysics and astrophysics, as well as in engineering. The specific effects related to rotating flows are predominantly a result of centripetal and Coriolis accelerations (Greenspan [1]), as well as, possibly, centrifugal buoyancy, as observed by Vadasz et al. [2]. The Coriolis effect and the resulting vortex formations have been identified theoretically as well as experimentally. Amar et al. [3] demonstrated the latter numerically as well as analytically and compared their results with experimental data. They focused on the separation between geostrophic flow and Ekman and Stewartson boundary layers. Asymptotic analyses of rotating flows identify Taylor–Proudman columns and two-dimensional flow at the leading order, and Ekman as well as Stewartson boundary layers for higher-order corrections [1], results that have been confirmed numerically as well as experimentally (Subbotin et al. [4], and Burmann and Noir [5]). An explanation for the appearance of von Kármán vortex streets around invisible bluff bodies, as captured by satellite images over certain islands in the Atlantic and Pacific Oceans, has been provided by Vadasz [6] in terms of Taylor–Proudman columns. Sarkar et al. [7] investigated the effects of a magnetic field on Taylor–Proudman columns in a rotating, electrically conducting fluid (MFD). They concluded that the "application of a magnetic field", "suppresses the Taylor column" in certain circumstances. In an electrically conducting fluid, the balance between the Coriolis acceleration and the Lorentz force is the mechanism that controls the Taylor–Proudman column. Extensive research

results on the problem of natural convection due to centrifugal buoyancy in rotating porous media have been presented by Vadasz et al. [8–11]. Vadasz [8] focused on the centrifugal buoyancy in a porous layer distant from the axis of rotation, and Vadasz [9] analyzed the Coriolis effect on a rotating porous layer heated from below via linear as well as weak nonlinear methods. Other investigations of centrifugal buoyancy in rotating porous media were performed by Saravanan and Vigneshwaran [12] and Kang et al. [13].

The effect of the magnetic field on the flow of conducting fluids has been studied extensively, e.g., identifying the law of isorotation (Allen et al. [14]). An analogy between the Taylor–Proudman theorem for rotating fluids and the law of isorotation for MFD might evolve as a consequence of the present paper's derivations.

The analogy between Coriolis and Lorentz forces is not new, e.g., the analogy between the gyrocompass and the magnetic compass was demonstrated by Opat [15]. In the present paper, it is demonstrated also for fluids as well as compasses.

The next section describes the analogy between rotating and magnetic (MFD) flows, followed by a theoretical demonstration of how electromagnetic columns are created when a flowing fluid carrying electric charges is exposed to an externally imposed magnetic field. The consequent two-dimensional magneto-eklinostrophic flow then emerges. Section 5 presents the fact that the conditions required for the electromagnetic columns and magneto-eklinostrophic flow to emerge are well satisfied in reality and should then be observable in lab experiments—e.g., [1], [2,3], or [4–6]. See the end of the document for further details on references. The terminology used for the "magneto-eklinostrophic" flow was originally intended to be magnetostrophic flow, in analogy to geostrophic flow, taken from the Greek combination of "geo" = of the earth and "strophē" = turning. Similarly, magnetostrophic should mean the flow "turning" around the virtual column due to magnetic rather than Coriolis effects due to the Earth's (geo) rotation. However, since the term "magnetostrophic" has already been commonly used in connection with magnetic effects on Taylor–Proudman Coriolis columns created by the Earth's rotation (e.g., King and Aurnou [16], Horn and Aurnou [17], Varma and Sreenivasan [18]), a different term was adopted here. Therefore, the adopted terminology for the type of flow created by an imposed magnetic field and the consequent electromagnetic columns is "magneto-eklinostrophic" (from Greek "ekklino" = deviate, and "strophē" = turning), to represent the deviation and turning of the flow around the object, as described in Section 3.

## 2. Analogy between Magneto-Fluid Dynamics (MFD/MHD) and Rotating Flows

The equations governing the isothermal compressible flow in a rotating frame of reference are the continuity and momentum equations, presented in the form of [1]:

$$\frac{\partial \rho}{\partial t} + \nabla \cdot (\rho \boldsymbol{V}) = 0 \tag{1}$$

$$\rho \left[ \frac{\partial \boldsymbol{V}}{\partial t} + (\boldsymbol{V} \cdot \nabla)\boldsymbol{V} + 2\boldsymbol{\omega} \times \boldsymbol{V} + \boldsymbol{\omega} \times (\boldsymbol{\omega} \times \boldsymbol{X}) \right] = -\nabla p + \rho \boldsymbol{g} + \mu \nabla^2 \boldsymbol{V} \tag{2}$$

where $\boldsymbol{V}(t, \boldsymbol{x}) = u\hat{\boldsymbol{e}}_x + v\hat{\boldsymbol{e}}_y + w\hat{\boldsymbol{e}}_z$ is the velocity vector; $\hat{\boldsymbol{e}}_x$, $\hat{\boldsymbol{e}}_y$, and $\hat{\boldsymbol{e}}_z$ are unit vectors in the $x, y$, and $z$ directions, respectively; $\boldsymbol{\omega} = \omega_x\hat{\boldsymbol{e}}_x + \omega_y\hat{\boldsymbol{e}}_y + \omega_z\hat{\boldsymbol{e}}_z$ is the constant angular velocity of rotation; $p$ is the pressure; $\mu$ is the dynamic viscosity; and $\boldsymbol{X} = x\hat{\boldsymbol{e}}_x + y\hat{\boldsymbol{e}}_y + z\hat{\boldsymbol{e}}_z$ is the position vector. These equations are the classical Navier–Stokes equations (Landau and Lifshitz [19]), where two additional acceleration terms due to rotation were added, namely, the centripetal acceleration term $\boldsymbol{\omega} \times (\boldsymbol{\omega} \times \boldsymbol{X})$ and the Coriolis acceleration term $2\boldsymbol{\omega} \times \boldsymbol{V}$ (Greenspan [1]). By assuming the fluid to be barotropic and using a linear relationship between pressure and density (this assumption applies to isothermal conditions for an ideal gas, and also approximately for isentropic conditions of the latter, and for liquids) the following equation can be used:

$$p = p_o + v_o^2(\rho - \rho_o) \tag{3}$$

where $v_o^2 = (\partial p/\partial \rho)_T$ or $v_o^2 = (\partial p/\partial \rho)_s$. Moving the Coriolis and centripetal terms to the right-hand side of the equation, and dividing Equation (2) by ρ, this yields:

$$\frac{\partial \boldsymbol{V}}{\partial t} + (\boldsymbol{V}\cdot\nabla)\boldsymbol{V} + = -\nabla\left(v_o^2 \ln\rho\right) - \boldsymbol{\omega} \times (\boldsymbol{\omega} \times \boldsymbol{X}) + \boldsymbol{g} + 2(\boldsymbol{V} \times \boldsymbol{\omega}) + \nu\nabla^2\boldsymbol{V} \tag{4}$$

where $\nu = \mu/\rho$ is the kinematic viscosity (note that despite the fact that in general the logarithm of a dimensional quantity is meaningless, the latter is still possible if it is the operand following a gradient operator, such as in Equation (4), where $v_o^2 =$ const. and $\nabla\left(v_o^2 \ln\rho\right) = v_o^2\nabla(\ln\rho) = v_o^2\nabla\rho/\rho$, which now becomes meaningful. Also, it becomes obvious now that one can divide and multiply this term by any constant density value, e.g., a characteristic scale, and then, the density becomes dimensionless, without affecting the equation at all). The centripetal acceleration term $\boldsymbol{\omega} \times (\boldsymbol{\omega} \times \boldsymbol{X})$ has a potential, and can be therefore moved under the gradient term in the form:

$$\frac{\partial \boldsymbol{V}}{\partial t} + (\boldsymbol{V}\cdot\nabla)\boldsymbol{V} + = -\nabla\left[v_o^2 \ln\rho + \frac{1}{2}(\boldsymbol{\omega} \times \boldsymbol{X})\cdot(\boldsymbol{\omega} \times \boldsymbol{X})\right] + \boldsymbol{g} + 2(\boldsymbol{V} \times \boldsymbol{\omega}) + \nu\nabla^2\boldsymbol{V} \tag{5}$$

It becomes appealing now to define a generalized reduced pressure term (a specific kinetic energy) in the form:

$$p_r = v_o^2 \ln\rho + \frac{1}{2}(\boldsymbol{\omega} \times \boldsymbol{X})\cdot(\boldsymbol{\omega} \times \boldsymbol{X}) \tag{6}$$

Substituting (6) into (5) leads to:

$$\frac{\partial \boldsymbol{V}}{\partial t} + (\boldsymbol{V}\cdot\nabla)\boldsymbol{V} + = -\nabla p_r + \boldsymbol{g} + 2(\boldsymbol{V} \times \boldsymbol{\omega}) + \nu\nabla^2\boldsymbol{V} \tag{7}$$

The momentum equation for an MFD fluid, i.e., a fluid that carries electric charges (even when, as a whole, it is neutrally charged), includes the electric and magnetic fields via the Lorentz force, and when neglecting the gravitational field—the latter being much weaker than the electromagnetic fields—can be presented in the form:

$$\rho\left[\frac{\partial \boldsymbol{V}}{\partial t} + (\boldsymbol{V}\cdot\nabla)\boldsymbol{V}\right] = -\nabla p + \rho_q\boldsymbol{E} + \rho_q(\boldsymbol{V} \times \boldsymbol{B_i}) + \mu\nabla^2\boldsymbol{V} \tag{8}$$

where $\boldsymbol{E}(t, x, y, z)$ is the electric field due to the distributed charges in the fluid, $\boldsymbol{V}$ is the velocity of the charges, and $\rho_q(\boldsymbol{V} \times \boldsymbol{B}_i)$ is the induced magnetic field that results from the electric current caused by the moving charges. When the fluid is exposed to an external magnetic field, an additional term in the form $\rho_q\left(\boldsymbol{V} \times \boldsymbol{B_f}\right)$ is to be added to Equation (8). See also Chandrasekhar et al. [20] for an equivalent form of this equation. Substituting Equation (3) into Equation (8), dividing Equation (8) by ρ, and using the definition of the generalized reduced pressure (6) for cases without rotation (i.e., $\boldsymbol{\omega} = 0$) produces:

$$\frac{\partial \boldsymbol{V}}{\partial t} + (\boldsymbol{V}\cdot\nabla)\boldsymbol{V} = -\nabla p_r + s_q\beta_q^{-1}\boldsymbol{E} + s_q\beta_q^{-1}(\boldsymbol{V} \times \boldsymbol{B_i}) + \nu\nabla^2\boldsymbol{V} \tag{9}$$

where $\beta_q = \rho/|\rho_q|$ is assumed to be constant and equal to the ratio between the total mass of the electric charges to the total electric charge, i.e., $\beta_q = \rho/|\rho_q| = m_q/|q|$, and

$$s_q = \begin{cases} 1 & \forall\ \rho_q > 0 \\ -1 & \forall\ \rho_q < 0 \end{cases} \tag{10}$$

is the electric charge sign function. Comparing Equation (9) for magnetic-fluid dynamic flow to Equation (7) for non-magnetic fluid dynamics in a rotating frame of reference, one observes the analogy when the gravitational field term $\boldsymbol{g}$ is replaced by the electric field term $s_q\beta_q^{-1}\boldsymbol{E}$, and the Coriolis acceleration term $2(\boldsymbol{V} \times \boldsymbol{\omega})$ is replaced by the magnetic term

$s_q\beta_q^{-1}(\boldsymbol{V}\times\boldsymbol{B_i})$. Consequently, it is plausible to anticipate that the magnetic field term $\boldsymbol{B_i}/\beta_q$ in MFD has an identical effect to the angular velocity of the rotation term $2\boldsymbol{\omega}$ in the Coriolis acceleration of the rotating flow. Note that even the units of $\boldsymbol{B_i}/\beta_q$ are $[\mathrm{TC/kg}] = \left[\mathrm{s}^{-1}\right]$, identical to the units of $\boldsymbol{\omega}$. Since the analogy between MFD flow and rotating flows was established by this comparison, one can therefore anticipate similar effects in MFD flow as those seen for the corresponding Coriolis effects of a rotating flow.

A similar analogy applies if the fluid is exposed to an externally imposed magnetic field. Then, Equation (9) takes the form:

$$\frac{\partial \boldsymbol{V}}{\partial t} + (\boldsymbol{V}\cdot\nabla)\boldsymbol{V} = -\nabla p_r + s_q\beta_q^{-1}\boldsymbol{E} + s_q\beta_q^{-1}(\boldsymbol{V}\times\boldsymbol{B_i}) + s_q\beta_q^{-1}\left(\boldsymbol{V}\times\boldsymbol{B_f}\right) + \nu\nabla^2\boldsymbol{V} \tag{11}$$

where $\boldsymbol{B_f} = B_f\hat{\boldsymbol{e}}_{\boldsymbol{f}}$ is the imposed magnetic field, which is constant, i.e., $B_f = \text{const.}$, and $\hat{\boldsymbol{e}}_{\boldsymbol{f}}$ is a unit vector in the direction of the imposed magnetic field.

## 3. Emerging Electromagnetic Columns in an Electrically Charged Fluid Flow Subject to an Imposed Magnetic Field

When the fluid is incompressible, or when the fluid can be assumed to be weakly compressible (i.e., the density does not change, but only when in a body force term in the momentum equation), the continuity Equation (1) transforms into:

$$\nabla\cdot\boldsymbol{V} = 0 \tag{12}$$

By considering a flow subject to an imposed magnetic field, Equation (11) can then be solved together with Maxwell equations, presented in the form:

*Coulomb law in field form*

$$\nabla\cdot\boldsymbol{E} = \frac{1}{\varepsilon_o}\rho_q \tag{13}$$

where $\varepsilon_o$ is the permittivity of the vacuum.

*Ampere law*

$$c_o^2\nabla\times\boldsymbol{B_i} = \frac{1}{\varepsilon_o}\rho_q\boldsymbol{V} + \frac{\partial \boldsymbol{E}}{\partial t} \tag{14}$$

where $c_o^2 = 1/\varepsilon_o\mu_o$ is the square of the speed of light in a vacuum, and $\mu_o$ is the permeability of the free space.

*Faraday law of induction*

$$\nabla\times\boldsymbol{E} = -\frac{\partial \boldsymbol{B_i}}{\partial t} \tag{15}$$

*Gauss law for the magnetic field*

$$\nabla\cdot\boldsymbol{B_i} = 0 \tag{16}$$

Note that $\boldsymbol{B_f}$ does not appear in Equations (14)–(16) because it is constant, and therefore its derivatives vanish.

Converting the equations into a dimensionless form requires the introduction of scales or characteristic values. The only requirement from such scales is that they are non-zero constants. Selecting $l_c$, $\rho_c$, $\rho_{qc} > 0$, $v_c$, $q_c > 0$, and $m$ as the length, mass density, charge density, velocity, electric charge, and mass scales, respectively, one can introduce the following additional scales in terms of the latter $t_c = l_c/v_c$, $\Delta p_c = \rho_c v_c^2$, $E_c = q_c/\varepsilon_o l_c^2$, $B_{ic} = \mu_o q_c^2/\left(m\varepsilon_o l_c^5\right)^{1/2}$, $B_{fc} = \left|\boldsymbol{B_f}\right| = B_f$. One can also relate the mass density scale to the mass scale, i.e., $\rho_c = m/l_c^3$, and the charge density scale to the charge scale, i.e., $\rho_{qc} = q_c/l_c^3$. By using these scales, the following dimensionless variables are defined as follows: $\boldsymbol{x}_* = \boldsymbol{x}/l_c$, $t_* = t\,v_c/l_c$, $\rho_* = \rho/\rho_c$, $\rho_{q*} = \rho_q/\rho_{qc}$, $v_* = v/v_c$, $p_* = p/\rho_c v_c^2$, $\boldsymbol{E}_* = \boldsymbol{E}\,\varepsilon_o l_c^2/q_c$, $\boldsymbol{B_{i*}} = \boldsymbol{B_i}\left(m\varepsilon_o l_c^5\right)^{1/2}/\mu_o q_c^2$, and $\boldsymbol{B_{f*}} = \hat{\boldsymbol{e}}_{\boldsymbol{f}}$. Substituting these dimensionless

variables into Equations (12) and (11) transforms the latter into the following dimensionless form:

$$\nabla_* \cdot \boldsymbol{V}_* = 0 \tag{17}$$

$$\frac{\partial \boldsymbol{V}_*}{\partial t_*} + (\boldsymbol{V}_* \cdot \nabla_*)\boldsymbol{V}_* = -\frac{1}{Ma^2}\nabla_* p_{r*} + \frac{s_q}{M_E}\boldsymbol{E}_* + \frac{s_q}{M_i^2}(\boldsymbol{V}_* \times \boldsymbol{B}_{i*}) + s_q M_B\left(\boldsymbol{V}_* \times \hat{\boldsymbol{e}}_f\right) + \frac{1}{Re}\nabla_*^2 \boldsymbol{V}_* \tag{18}$$

where the following dimensionless groups emerge:

- **the Mach number**

$$Ma = \frac{v_c}{v_o} \tag{19}$$

- **the electric field number**

$$M_E = \frac{\beta_q l_c v_c^2 \varepsilon_o}{q_c} \tag{20}$$

- **the induced magnetic field number**

$$M_i^2 = \frac{\beta_q v_c \left(m\,\varepsilon_o l_c^3\right)^{1/2}}{\mu_o q_c^2} \tag{21}$$

- **the imposed magnetic field number**

$$M_B = \frac{B_f l_c}{\beta_q v_c} \tag{22}$$

- **the Reynolds number**

$$Re = \frac{v_c l_c}{\nu} \tag{23}$$

Dividing Equation (18) by $M_B$ produces (after dropping the symbol *, as now all variables are dimensionless):

$$Ro_M \frac{\partial \boldsymbol{V}}{\partial t} + Ro_M(\boldsymbol{V}\cdot\nabla)\boldsymbol{V} = -\nabla \widetilde{p}_r + \frac{s_q}{M_B M_E}\boldsymbol{E} + \frac{s_q}{M_B M_i^2}(\boldsymbol{V} \times \boldsymbol{B}_i) + s_q\left(\boldsymbol{V} \times \hat{\boldsymbol{e}}_f\right) + Ek_M \nabla^2 \boldsymbol{V} \tag{24}$$

where a rescaled pressure is introduced in the form $\widetilde{p}_r = p_r / M_B Ma^2$, and where new dimensionless groups emerge as follows:

- **the magnetic Rossby number**

$$Ro_M = M_B^{-1} = \frac{l_c}{\left(B_f/\beta_q\right)v_c} \tag{25}$$

- **the magnetic Ekman number**

$$Ek_M = M_B^{-1} Re^{-1} = \frac{\nu}{\left(B_f/\beta_q\right)l_c^2} \tag{26}$$

A steady state and $M_B >> 1$ is assumed, which implies $Ro_M << 1$. Then, if $Re = O(1)$ (or $Re >> 1$) is also assumed, which implies $Ek << 1$; if $M_E = O(1)$ (or $M_E >> 1$); and if $M_i^2 = O(1)$ (or $M_i^2 >> 1$), then neglecting the terms in Equation (24) corresponding to the small coefficients leads to:

$$\hat{\boldsymbol{e}}_f \times \boldsymbol{V} = -\nabla\left(s_q \widetilde{p}_r\right) \tag{27}$$

since $s_q = 1/s_q$, by definition, as presented in Equation (10). Selecting the coordinates axes in a such a way that the direction of the imposed magnetic field $\boldsymbol{B}_f$ is aligned with the negative direction of the $z$-axis, i.e., $\hat{\boldsymbol{e}}_f = -\hat{\boldsymbol{e}}_z$, transforms (27) into:

$$\hat{\boldsymbol{e}}_z \times \boldsymbol{V} = \nabla\left(s_q \tilde{p}_r\right) \tag{28}$$

Taking the curl ($\nabla\times$) of Equation (28) produces:

$$\nabla \times \left(\hat{\boldsymbol{e}}_z \times \boldsymbol{V}\right) = 0 \tag{29}$$

However, using Equation (17) and evaluating the curl in (29) leads to:

$$\nabla \times \left(\hat{\boldsymbol{e}}_z \times \boldsymbol{V}\right) = -\left(\hat{\boldsymbol{e}}_z \cdot \nabla\right)\boldsymbol{V} = 0 \tag{30}$$

Evaluating the dot product yields:

$$\left(\hat{\boldsymbol{e}}_z \cdot \nabla\right)\boldsymbol{V} = \frac{\partial \boldsymbol{V}}{\partial z} = 0 \tag{31}$$

Equation (31) is the electromagnetic equivalent to the Taylor–Proudman theorem for rotating flows. This equation represents the conclusion that the velocity at the leading order cannot change in the direction of the imposed magnetic field. Chandrasekhar [20] arrived at the same conclusion for a stationary fluid subject to small perturbations in velocity and magnetic field. Here, the latter is shown for a moving fluid subject to an imposed magnetic field. It implies, in particular, that $\partial w/\partial z = 0$, and since $w = 0$ at $z = 0$ due to impermeability boundary conditions, this means that $w = 0$ for all values of $z$. This indicates that a flow over an object aligning with the imposed magnetic field, as presented in Figure 1, is impossible, because it introduces a vertical component of velocity, $w \neq 0$, and consequently violates Equation (31). The conclusion is that the flow will adjust around the object, as presented in Figure 2a.

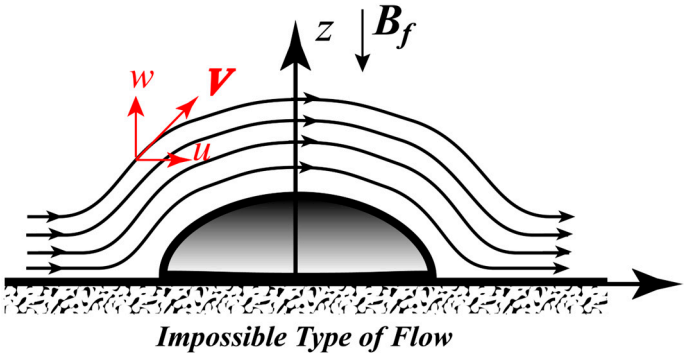


**Figure 1.** An impossible type of flow above a small object, aligned with the magnetic field.

However, this flow pattern is also independent of $z$, because Equation (31) implies that

$$\frac{\partial \boldsymbol{V}}{\partial z} = 0 \quad \Rightarrow \quad \frac{\partial u}{\partial z} = \frac{\partial v}{\partial z} = \frac{\partial w}{\partial z} = 0 \tag{32}$$

Consequently, the flow pattern extends over the whole height, creating a fluid column above the object that behaves like a solid body, as presented in Figure 2b. These results are correct for a leading order approximation in the bulk. A higher-order evaluation should reveal a magnetic Ekman boundary layer in order to satisfy the non-slip boundary condition at $z = 0$.

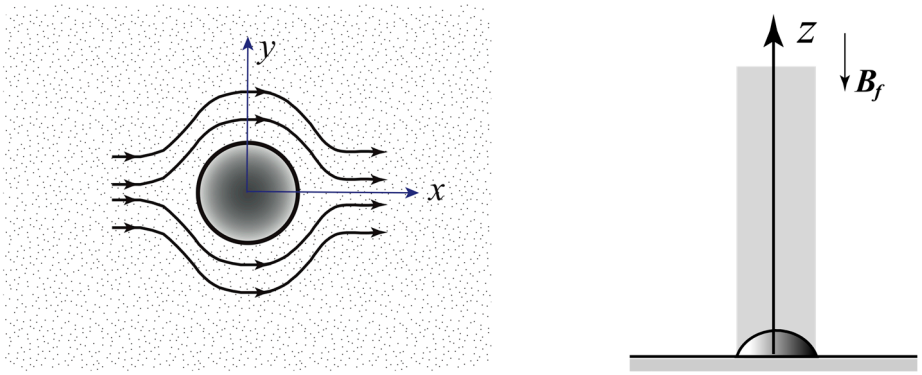


(**a**) (**b**)

**Figure 2.** (**a**) The flow will adjust around the object; (**b**) The flow pattern extends over the whole height, creating a fluid column above the object, which behaves like a solid body.

## 4. Magneto-eklinostrophic Flow

The lack of a vertical component of velocity leads to two-dimensional flow, at which point, it becomes appealing to introduce a stream function that causes the continuity Equation (17) to be identically satisfied, i.e.,

$$u = -\frac{\partial \psi}{\partial y};\ v = \frac{\partial \psi}{\partial x};\ w = 0 \tag{33}$$

Substituting (33) into Equation (28) after determining the vector product on its left-hand side produces:

$$\nabla_H \psi = \nabla_H \left( s_q \widetilde{p}_r \right) \tag{34}$$

where $\nabla_H = \partial/\partial x \hat{\boldsymbol{e}}_{\boldsymbol{x}} + \partial/\partial y \hat{\boldsymbol{e}}_{\boldsymbol{y}}$ is the horizontal gradient operator.

As both the generalized reduced pressure $\widetilde{p}_r$ and the stream function $\psi$ can be related to an arbitrary reference value, the conclusion from (34) is that the stream function and the generalized reduced pressure are the same within the limits of small magnetic Ekman and Rossby numbers. This type of magneto-eklinostrophic flow (in analogy to the geostrophic type in rotating flows) means that isobars represent streamlines at the leading order for $Ek_M << 1$ and $Ro_M << 1$, i.e., for $M_B >> 1$.

## 5. Parameter Estimation and Suggested Experimental Setup

In this section, an evaluation of the conditions required for electromagnetic columns and magneto-eklinostrophic flow to exist are tested via parameter estimation, and a suggested experimental setup is proposed. The objective is to establish the criteria for theoretical results to be detectable in practice. The main condition for the emergence of electromagnetic columns and magneto-eklinostrophic flow was derived as:

$$M_B >> 1 \ \Rightarrow\ \frac{v_c}{\left( B_f/\beta_q \right) l_c} << 1 \ \Rightarrow\ \frac{B_f}{\beta_q} >> \frac{v_c}{l_c} \tag{35}$$

For the flow of free charges, one can estimate the value of $\beta_q \approx m_e/|e| = 5.7{\cdot}10^{-12}$ [kg/$C$] as the ratio between the mass of the elementary charge (the electron) and the absolute value of its electrical charge. For flow of charges via fluids, one has to account for the mass of the fluid too when evaluating the mass; however, for rarified gases, the former estimation still applies as an approximation. Then, for an imposed magnetic field of $B_f = 1$ [T], the ratio $B_f/\beta_q \cong 1.75{\cdot}10^{11}$ [s$^{-1}$] and condition (35) implies $(v_c/l_c) << 1.75{\cdot}10^{11}$ [s$^{-1}$]. This means that for length scales of $l_c = 1$[m], $l_c = 10^{-2}$[m], and $l_c = 10^{-3}$[m], the conditions that the average fluid velocity should satisfy are $v_c << 1.75{\cdot}10^{11}$ [m/s], $v_c << 1.75{\cdot}10^{9}$ [m/s], and $v_c << 1.75{\cdot}10^{8}$ [m/s], respectively. The first two values exceed the speed of light in a

vacuum. These conditions are easily satisfied in any realistic experimental setups. Even if the value of $\beta_q$ turns out to be much larger, even by a few orders of magnitude, it should not be difficult to satisfy these conditions, which in extreme cases will require stronger magnetic fields. The estimates for the secondary conditions, i.e., $Re = O(1)$ (or $Re >> 1$), $M_E = O(1)$ (or $M_E >> 1$), or $M_i^2 = O(1)$ (or $M_i^2 >> 1$), indicate that they can also be satisfied in reality. For example, for plasmas, large velocities are required, such that for length scales of $l_c = 1$ [m], $l_c = 10^{-2}$ [m], and $l_c = 10^{-3}$[m], the condition that the average fluid velocity should satisfy when combined with the condition for $M_B >> 1$ is $1.75{\cdot}10^{11}$ [m/s] $>> v_c >> 1.2{\cdot}10^3$ [m/s], $1.75{\cdot}10^9$ [m/s] $>> v_c >> 1.2{\cdot}10^5$ [m/s], and $1.75{\cdot}10^8$ [m/s] $>> v_c >> 1.2{\cdot}10^6$ [m/s], respectively. For liquid metals, the conditions are much less constrained, as $1.75{\cdot}10^{11}$ [m/s] $>> v_c >> 10^{-7}$ [m/s], $1.75{\cdot}10^9$ [m/s] $>> v_c >> 10^{-7}$ [m/s], and $1.75{\cdot}10^8$ [m/s]$>> v_c >> 10^{-4}$ [m/s]. Therefore, experiments to confirm the emergence of electromagnetic columns and magneto-eklinostrophic flow are suggested and planned using the constraints evaluated in this section and an experimental setup, as described in Figures 1 and 2, and in detail in Figure 3. Using earth magnets for creating the imposed magnetic field is also quite practical given the estimated parameter values. An imposed magnetic field is anticipated to affect streams of beams of charges or the MFD-type fluids that flow through. A specific type of detection via a tracer, PIV, or optical methods such as interferometry or similar can be used for the detection of the flow of charges. When magneto-eklinostrophic flow and magnetic virtual columns are detected, this raises the possibility of the creation of von Kármán vortex streets, as presented in Figure 3 in a "top view". This is similar to the creation of von Kármán vortex streets in the wake of Taylor–Proudman columns in rotating flows, as captured by satellite images and presented theoretically by Vadasz et al. [6].

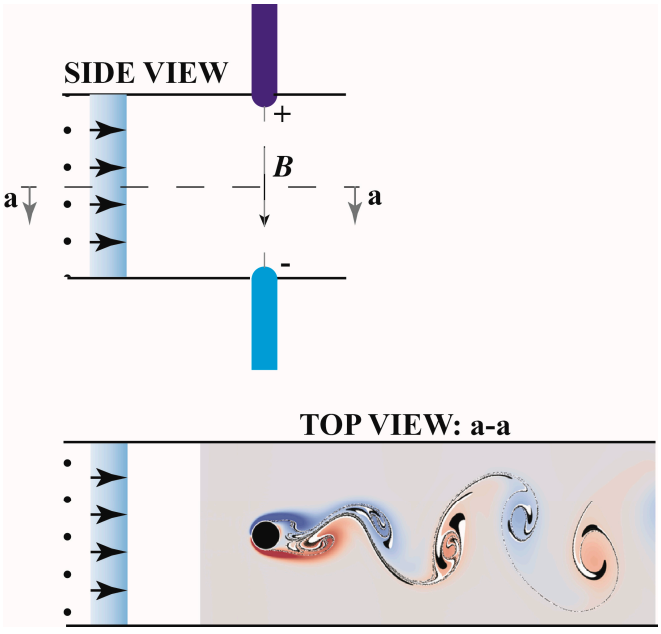


**Figure 3.** Proposed experimental set-up: An imposed magnetic field affecting a stream of beams of charges or MFD type fluids. (the top view von Kármán vortex streets, courtesy of Andrew Yeckel, PhD https://andrewyeckel.com).

## 6. Conclusions

A theoretical derivation identifying an analogy between magneto-fluid dynamics (MFD/MHD) and geostrophic flow in a rotating frame of reference is presented here. The latter includes the existence of electromagnetic columns identical to Taylor–Proudman columns. The emergence of these columns is conditional upon very small magnetic Rossby numbers or, alternatively, very large values of its reciprocal, the electromagnetic number, as well as small values of the magnetic Ekman number, which translates into a Reynolds number that is $O(1)$. These conditions were shown to be possible to satisfy in reality. As a

result, the electromagnetic fluid flow is two dimensional, and the streamlines are shown to be identical to the pressure lines, in complete analogy to rotating geostrophic flows. Then, von Kármán vortices are anticipated in the wake of the virtual magnetic columns. A possible setup is suggested to confirm the theoretical results experimentally.

**Funding:** This research received no external funding.

**Data Availability Statement:** The original contributions presented in the study are included in the article, further inquiries can be directed to the corresponding author.

**Conflicts of Interest:** The author declares no conflicts of interest.

## Nomenclature

| | |
|---|---|
| $\boldsymbol{B_i}$ | the induced magnetic field [T] = [N s/C m], |
| $\boldsymbol{B_f} = B_f \hat{\boldsymbol{e}}_f$ | the imposed magnetic field [T] = [N s/C m], |
| $c_o = 1/\sqrt{\varepsilon_o \mu_o}$ | speed of light in vacuum [m/s], |
| $\hat{\boldsymbol{e}}_f$ | unit vector in the direction of the imposed magnetic field [dim-less], |
| $\hat{\boldsymbol{e}}_x, \hat{\boldsymbol{e}}_y, \hat{\boldsymbol{e}}_z$ | unit vectors in the $x, y$, and $z$ directions, respectively, [dim-less], |
| $\boldsymbol{E}$ | electric field [N/C], |
| $E_c$ | characteristic electric field [N/C], |
| $\boldsymbol{g}$ | acceleration due to gravity [m/s$^2$], |
| $l_c$ | characteristic length scale [m], |
| $m$ | characteristic mass scale [kg], |
| $Ma = v_c/v_o$ | Mach number, a ratio between the characteristic velocity and the speed of pressure wave propagation [dim-less], |
| $M_B = B_f l_c/\beta_q v_c$ | imposed magnetic field number [dim-less], |
| $M_E = \beta_q l_c v_c^2 \varepsilon_o / q_c$ | electric field number [dim-less], |
| $M_i^2 = \beta_q v_c \left(m\, \varepsilon_o l_c^3\right)^{1/2} / \mu_o q_c^2$ | induced magnetic field number [dim-less], |
| $p$ | pressure, |
| $p_r = v_o^2 \ln \rho + \frac{1}{2}(\boldsymbol{\omega} \times \boldsymbol{X}) \cdot (\boldsymbol{\omega} \times \boldsymbol{X})$ | reduced pressure [m$^2$/s$^2$ = Pa/(kg/m$^3$)], |
| $q_c$ | characteristic charge scale [C], |
| $Re = v_c l_c/\nu$ | Reynolds number [dim-less], |
| $Ro_M = M_B^{-1} = l_c/\left(B_f/\beta_q\right) v_c$ | magnetic Rossby number [dim-less], |
| $s_q = \left(1 \ \ \forall\, \rho_q > 0\right)$ or $\left(-1 \ \ \forall\, \rho_q < 0\right)$ | electric charge sign function [dim-less], |
| $t$ | time [s], |
| $u$ | the component of the velocity in the $x$ direction [m/s], |
| $v$ | the component of the velocity in the $y$ direction [m/s], |
| $\boldsymbol{V}(t, \boldsymbol{x}) = u\hat{\boldsymbol{e}}_x + v\hat{\boldsymbol{e}}_y + w\hat{\boldsymbol{e}}_z$ | velocity vector [m/s], |
| $v_c$ | characteristic velocity scale [m/s], |
| $v_o = \sqrt{(\partial p/\partial \rho)_T}$ or $v_o = \sqrt{(\partial p/\partial \rho)_S}$ | speed of pressure wave propagation, inversely proportional to the compressibility of the fluid [m/s], |
| $w$ | the component of the velocity in the $z$ direction [m/s], |
| $\boldsymbol{X} = x\hat{\boldsymbol{e}}_x + y\hat{\mathbf{e}}_y + z\hat{\boldsymbol{e}}_z$ | position vector to any point in the flow domain [m], |
| Greek Symbols | |
| $\beta_q = \rho/\rho_q$ | mass density to charge density ratio [kg/C], |
| $\varepsilon_o$ | permittivity of vacuum [F/m] = [C$^2$/N m$^2$], |
| $\mu_o$ | permeability of free space [H/m] = [N s$^2$/C$^2$], |
| $\mu$ | dynamic viscosity [Pa s], |
| $\nu = \mu/\rho$ | kinematic viscosity [m$^2$/s], |
| $\boldsymbol{\omega} = \omega_x \hat{\boldsymbol{e}}_x + \omega_y \hat{\boldsymbol{e}}_y + \omega_z \hat{\boldsymbol{e}}_z$ | constant angular velocity of rotation vector [s$^{-1}$], |
| $\rho$ | mass density [kg/m$^3$], |
| $\rho_q$ | charge density [C/m$^3$], |

## References


1. Greenspan, H.P. *Theory of Rotating Fluids*; Cambridge University Press: Cambridge, UK, 1968.
2. Vadasz, P. Centrifugal buoyancy in a rotating fluid layer next to and distant from the rotation axis. *Phys. Fluids* **2021**, *33*, 034123. [CrossRef]
3. Amar, S.D.; Rashkovan, A.; Ziskind, G. Analysis of a stable bathtub vortex in a rotating container. *Phys. Fluids* **2023**, *35*, 037124. [CrossRef]
4. Subbotin, S.; Shmakova, N.; Kozlov, V.; Ermanyuk, E. Nonlinear regimes of inertial wave attractors generated by a precessing lid: Zonal flows and Rossby waves. *Phys. Fluids* **2023**, *35*, 074110. [CrossRef]
5. Burmann, F.; Noir, J. Effects of bottom topography on the spin-up in a cylinder. *Phys. Fluids* **2018**, *30*, 106601. [CrossRef]
6. Vadasz, P. von Kármán vortex streets around invisible bluff bodies. *Phys. Fluids* **2023**, *35*, 096604. [CrossRef]
7. Sarkar, S.; Sahoo, B.; Sekhar, T.V.S. Influence of magnetic field in the control of Taylor column phenomenon in the translation of a sphere in a rotating fluid. *Phys. Fluids* **2021**, *33*, 073606. [CrossRef]
8. Vadasz, P. Stability of Free Convection in a Rotating Porous Layer Distant from the Axis of Rotation. *Transp. Porous Media* **1996**, *23*, 153–173. [CrossRef]
9. Vadasz, P. Coriolis Effect on Gravity Driven Convection in a Rotating Porous Layer Heated from Below. *J. Fluid Mech.* **1998**, *376*, 351–375. [CrossRef]
10. Vadasz, P. *Fluid Flow and Heat Transfer in Rotating Porous Media*; Springer Briefs in applied Science and Engineering; Springer: Cham, Switzerland, 2016; ISBN 978-3-319-20055-2 (Print), 978-3-319-20056-9 (Online).
11. Vadasz, P. Instability and Convection in Rotating Porous Media: A Review. *Fluids* **2019**, *4*, 147. [CrossRef]
12. Saravanan, S.; Vigneshwaran, S. Centrifugal filtration convection in bidisperse media. *Phys. Fluids* **2020**, *32*, 084109. [CrossRef]
13. Kang, J.; Chen, X.; Fu, C.; Tan, W. Centrifugally driven thermal convection in a rotating porous cylindrical annulus. *Phys. Fluids* **2013**, *25*, 044104. [CrossRef]
14. Allen, J.E.; Auer, P.L.; Endean, V.G. On the Law of Isorotation and Laboratory Experiments. *Plasma Phys.* **1976**, *18*, 143–154. [CrossRef]
15. Opat, G.I. Coriolis and Magnetic Forces: The Gyrocompass and Magnetic Compass as Analogs. *Am. J. Phys.* **1990**, *58*, 1173–1176. [CrossRef]
16. King, E.M.; Aurnou, M. Magnetostrophic balance as the optimal state for turbulent magnetoconvection. *Proc. Natl. Acad. Sci. USA* **2015**, *112*, 990–994. [CrossRef]
17. Horn, S.; Aurnou, M. The Elbert range of magnetostrophic convetion. I. Linear Theory. *Proc. R. Soc. A* **2022**, *478*, 20220313. [CrossRef]
18. Varma, A.; Sreenivasan, B. The role of low magnetostrophic waves in the formation of the axial dipole in planetary dynamos. *Phys. Earth Planet. Inter.* **2022**, *333*, 106944. [CrossRef]
19. Landau, L.D.; Lifshitz, E.M. Fluid Mechanics. In *Course of Theoretical Physics*; Pergamon Press: Oxford, UK; New York, NY, USA; Toronto, ON, Canada; Sydney, Australia; Paris, France; Frankfurt, Germany, 1959; Volume 6.
20. Chandrasekhar, S. *Hydrodynamic and Hydromagnetic Stability*; Oxford University Press: Oxford, UK; Dover Publications, Inc.: Mineola, NY, USA, 1961.


**Disclaimer/Publisher's Note:** The statements, opinions and data contained in all publications are solely those of the individual author(s) and contributor(s) and not of MDPI and/or the editor(s). MDPI and/or the editor(s) disclaim responsibility for any injury to people or property resulting from any ideas, methods, instructions or products referred to in the content.